J Neurophysiol 113: 1275–1282, 2015.
First published November 26, 2014; doi:10.1152/jn.00629.2014.

Microchip amplifier for in vitro, in vivo, and automated whole cell patch-clamp recording

Reid R. Harrison,[1] Ilya Kolb,[2] Suhasa B. Kodandaramaiah,[3,4] Alexander A. Chubykin,[5] Aimei Yang,[3] Mark F. Bear,[6] Edward S. Boyden,[3,4]* and Craig R. Forest[7]*

[1]*Intan Technologies, Los Angeles, California;* [2]*Wallace H. Coulter Department of Biomedical Engineering, Georgia Institute of Technology, Atlanta, Georgia;* [3]*Media Lab, Massachusetts Institute of Technology, Cambridge, Massachusetts;* [4]*McGovern Institute, Massachusetts Institute of Technology, Cambridge, Massachusetts;* [5]*Department of Biological Sciences, Purdue University, West Lafayette, Indiana;* [6]*Howard Hughes Medical Institute, The Picower Institute for Learning and Memory, Department of Brain and Cognitive Sciences, Massachusetts Institute of Technology, Cambridge, Massachusetts; and* [7]*George W. Woodruff School of Mechanical Engineering, Georgia Institute of Technology, Atlanta, Georgia*

Submitted 21 August 2014; accepted in final form 21 November 2014

Harrison RR, Kolb I, Kodandaramaiah SB, Chubykin AA, Yang A, Bear MF, Boyden ES, Forest CR. Microchip amplifier for in vitro, in vivo, and automated whole cell patch-clamp recording. *J Neurophysiol* 113: 1275–1282, 2015. First published November 26, 2014; doi:10.1152/jn.00629.2014.—Patch clamping is a gold-standard electrophysiology technique that has the temporal resolution and signal-to-noise ratio capable of reporting single ion channel currents, as well as electrical activity of excitable single cells. Despite its usefulness and decades of development, the amplifiers required for patch clamping are expensive and bulky. This has limited the scalability and throughput of patch clamping for single-ion channel and single-cell analyses. In this work, we have developed a custom patch-clamp amplifier microchip that can be fabricated using standard commercial silicon processes capable of performing both voltage- and current-clamp measurements. A key innovation is the use of nonlinear feedback elements in the voltage-clamp amplifier circuit to convert measured currents into logarithmically encoded voltages, thereby eliminating the need for large high-valued resistors, a factor that has limited previous attempts at integration. Benchtop characterization of the chip shows low levels of current noise [1.1 pA root mean square (rms) over 5 kHz] during voltage-clamp measurements and low levels of voltage noise (8.2 μV rms over 10 kHz) during current-clamp measurements. We demonstrate the ability of the chip to perform both current- and voltage-clamp measurement in vitro in HEK293FT cells and cultured neurons. We also demonstrate its ability to perform in vivo recordings as part of a robotic patch-clamping system. The performance of the patch-clamp amplifier microchip compares favorably with much larger commercial instrumentation, enabling benchtop commoditization, miniaturization, and scalable patch-clamp instrumentation.

electrophysiology; patch clamp; electronics; in vivo; in vitro

PATCH-CLAMP ELECTROPHYSIOLOGY has been a central tool of neuroscience and pharmaceutical research since its advent in the late 1970s (Neher and Sakmann 1976). The technique of patch clamping utilizes glass micropipettes and sensitive analog electronics to monitor the synaptic currents and intracellular voltages of individual excitable cells. This is accomplished by using micromanipulators to guide a fine micropipette tip into contact with a cell's membrane to create a tight physical connection (or "gigaseal") between the tip of the pipette and the cell membrane. If necessary, it is possible to apply suction pulses to "break in" through the membrane and gain access to the cell cytoplasm, creating a "whole cell" configuration (Hamill et al. 1981; Margrie et al. 2002; Molleman 2002). Ultra low-noise microelectrode amplifiers are then used to monitor and manipulate the cell's picoamp-scale current signals and millivolt-scale voltage signals. Feedback circuitry within the patch-clamp amplifier can enable the user to hold the cell's membrane voltage constant while monitoring the ionic current flux in and out of the cell using a technique known as voltage clamp (Safronov and Vogel 1999). In neuroscience, the voltage-clamp technique has been used extensively to characterize basic biophysical properties of neurons (Hodgkin and Huxley 1952). Alternatively, the user may perform a "current-clamp" experiment: injecting current into the cell to observe voltage fluctuations such as action potentials and low-amplitude subthreshold events.

In this article we report on the development and testing of a custom patch-clamp microchip, or "PatchChip," that performs the functions of a traditional patch-clamp electrophysiology rig but is much smaller and lighter and requires lower power. Whereas a traditional patch-clamp amplifier consists of a head stage connected to a rack-mounted amplifier/acquisition unit with a cable carrying sensitive analog signals, PatchChip incorporates all amplifier functions in one small device and requires only a small number of additional components on the head stage circuit board to produce a robust digital signal that interfaces to a host computer via a USB adapter. All amplifier control is performed through a software graphical user interface (GUI).

MATERIALS AND METHODS

Voltage-clamp design. A simplified circuit schematic of a traditional patch-clamp amplifier for whole cell voltage-clamp experiments is shown in Fig. 1 (Molleman 2002; Sakmann and Neher 2009). In voltage-clamp mode, an operational amplifier ("op amp") is used in a feedback loop to hold or "clamp" the cell membrane potential to a user-specified value (V_{clamp}). An op amp with field effect transistor (FET) inputs is used in these applications to ensure that current flowing into the input terminals will be less than a picoamp in magnitude (Sakmann and Neher 2009; Sigworth 1995). Thus the whole cell current (I_{cell}), resulting from the sum of all ion channel activity in the cell membrane, is forced through one of the feedback

* E. S. Boyden and C. R. Forest contributed equally to this work.

Address for reprint requests and other correspondence: R. Harrison, Intan Technologies, LLC, 8726 S. Sepulveda Blvd., Suite D2121, Los Angeles, CA 90045.

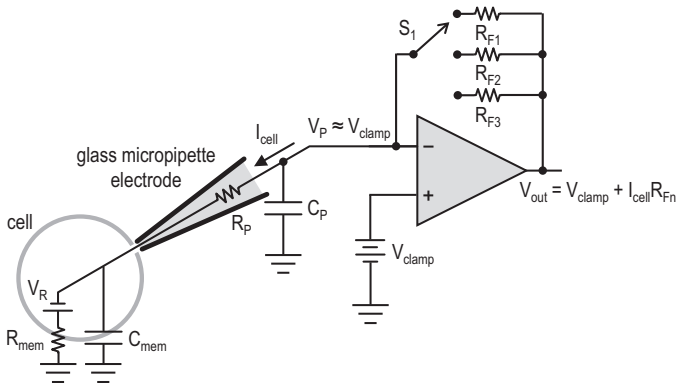

Fig. 1. A simplified schematic of a traditional patch-clamp amplifier in voltage-clamp mode. A field effect transistor (FET)-input operational amplifier (op amp) uses feedback to hold the pipette voltage (V_P) at the user-specified potential (V_{clamp}). The whole cell current (I_{cell}) passes through feedback resistor R_{Fn}, selected by switch S_1. The resulting output voltage (V_{out}) is linearly proportional to the measured current. Several different feedback resistors are needed to accurately measure different current ranges from picoamps to nanoamps. These resistors must be in the high mega- and gigaseal range, making them relatively large and impractical to integrate on a chip. See text for definition of variables.

resistors (R_{Fn}), converting the current into a linearly proportional voltage that is digitized by an analog-to-digital converter (ADC) and sent to a computer for analysis and storage. The properties of various types of ion channels are studied by methodically sweeping V_{clamp} over a range of roughly ±100 mV and monitoring the magnitude and time course of the resulting whole cell currents. Additional circuits not shown in Fig. 1 compensate for the resistance (R_P) and capacitance (C_P) of the pipette.

Since the resulting output voltage (V_{out}) is equal to $I_{cell}R_F$ (after the known voltage V_{clamp} has been subtracted), a value of R_F must be selected that scales tiny picoamp or nanoamp currents to a convenient voltage for ADCs: millivolts or volts. This requires extremely high-valued resistors in the range of 10 MΩ to 50 GΩ. Since currents can vary widely (e.g., 10–50 pA with a single synapse active; 2–3 nA with many synapses active), a bank of resistors with a broad range of R_F values is required, and the user must select a range that provides good resolution without overloading the ADC. Building circuit boards for measuring picoamp currents is challenging: contamination from a fingerprint or residual solder flux can create parasitic gigaohm-level resistances that short out R_F components; large-feedback resistors must be protected from surface oxidation or moisture. Integrating the critical feedback elements on the same chip as the op amp would reduce the size and cost of these circuits.

Recent work has integrated the traditional patch-clamp amplifier shown in Fig. 1 in a 0.5-μm silicon-on-sapphire complementary metal-oxide semiconductor (CMOS) fabrication process (Goldstein et al. 2011; Laiwalla et al. 2006; Weerakoon et al. 2010). It is difficult to create large-valued resistors on a chip: there are typically only one or two types of resistive material available, so to create higher resistances, the only option is to create longer and longer serpentine traces of resistive material. This resistive material is deposited on a thin insulating layer covering the underlying silicon wafer, so larger resistors have larger parasitic capacitances to the chip substrate, which can cause stability problems in feedback loops. Limited chip area and undesirable stray capacitances make it difficult to build high-quality on-chip resistors in the high-megaohm range. Previous research efforts managed to integrate resistors in the range of 10–100 MΩ onto chips, but this is at the low end of feedback resistances used in traditional patch-clamp amplifiers, and the ability to resolve small currents suffered as a result. A current noise floor of 8 pA rms over a 10-kHz bandwidth was reported (Weerakoon et al. 2010). In comparison, commercial voltage-clamp systems have current noise floors more than 10 times lower over equivalent bandwidths (Molecular Devices 2014a, 2014b).

To achieve higher sensitivity with a fully integrated patch-clamp amplifier, we designed and simulated a novel voltage-clamp circuit architecture that eliminates the need for very large feedback resistors. The circuit, shown in simplified form in Fig. 2*A*, uses on-chip diode-like circuit elements in the feedback path in place of resistors. Diodes have an exponential current-voltage relationship when they are forward biased; the forward current through the diode (i_D) is an exponential function of the voltage across the diode (v_D):

$$i_D = I_S\left(e^{v_D/(nV_T)} - 1\right) \approx I_S e^{v_D/(nV_T)}$$

for $v_D > 0$, where I_S is a device constant with units of current, n is a constant approximately equal to 1.5, and V_T is the thermal voltage kT/q, which is ~26 mV at room temperature. When $v_D < 0$, the diode current approaches I_S, which is far below 1 pA, so we can consider the reverse current to be practically zero. By placing two anti-parallel diode-like devices D_1 and D_2 [actually subthreshold FETs (Mead 1989; Vittoz and Fellrath 1977)] in the feedback loop as shown in Fig. 2, we ensure that one of the devices is always on and the other off, depending on the direction of I_{cell}. By placing the diodes in a feedback loop, we invert the exponential current-voltage relationship and produce an output voltage that is a logarithmic function of the measured current I_{cell}:

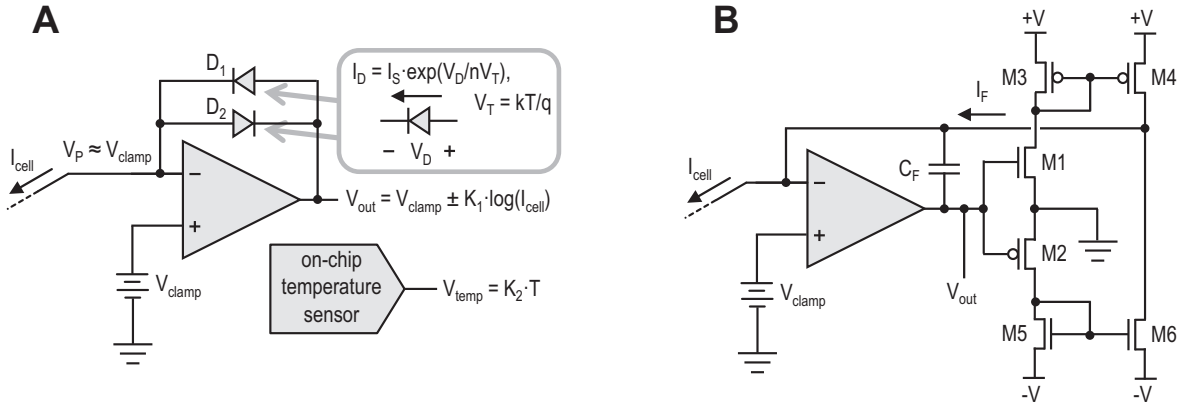

Fig. 2. *A*: simplified schematic of the voltage-clamp circuitry in PatchChip. On-chip diodes are used in place of large-valued feedback resistors. Diodes have an exponential relationship between voltage and current, as well as a sensitivity to temperature. Depending on the direction of I_{cell}, either D_1 or D_2 will conduct, and V_{out} will be a logarithmic function of the measured current. An on-chip temperature sensor can be used to factor out temperature dependencies. *B*: detailed schematic of voltage-clamp circuit showing transistors M1–M6 that implement the diode-like feedback elements. See text for definition of variables.

$$V_{out} = V_{clamp} \pm nV_T \ln \frac{|I_{cell}|}{I_S},$$

where the sign depends on the direction of current. The output voltage encodes a signed, logarithmically compressed measure of cell current. This representation has significant advantages for voltage-clamp applications: it allows a wide range of currents (ranging from picoamps to microamps), both positive and negative, to be represented in a limited voltage range that is compatible with an analog-to-digital converter (ADC). Relative current changes are encoded as constant voltage steps; the entire range of currents from 1 pA to 1 μA encompasses a voltage range of only 0.54 V. After V_{out} is sampled with a standard 16-bit ADC, relative current changes of $<0.1\%$ will be discernible across this entire range. Cellular currents spanning many orders of magnitudes can be measured without having to switch between different feedback resistors.

The current-voltage relationship of the diode-like elements is affected by ambient temperature: V_T is proportional to temperature, and I_S, too, varies with temperature. To address this problem, we integrated an on-chip temperature sensor (Tuthill 1998) near the diodes (Fig. 2*A*). A calibration is performed for both diodes to resolve their individual dependence on temperature and correct for it. Their temperature dependence does not vary over time; thus the calibration step only needs to be performed once for each PatchChip device. This calibration is then used to factor out diode temperature dependencies in software. The software also converts the logarithmically encoded output voltage into a linear measure of current for display and recording, and performs a self-calibration of the voltage-clamp circuits upon power-up.

Figure 2*B* shows a detailed schematic of the voltage-clamp circuit. Transistors M1 and M2 operate in subthreshold mode and act like diodes, producing a current that is an exponential function of V_{out}. For positive values of V_{out}, M1 is active and M2 is off; for negative values of V_{out}, M2 is active and M1 is off. The current mirrors M3–M4 and M5–M6 redirect these currents and produce a feedback current, I_F. The op amp drives V_{out} to a value that equalizes I_F and I_{cell}. The feedback capacitor C_F ensures that the feedback loop comprising the op amp and transistors M1–M6 remains stable.

Current-clamp design. The majority of patch-clamp experiments use the voltage-clamp configuration to hold a membrane potential and measure the resulting currents. However, many experiments require use of the current-clamp configuration, where a constant current is injected into the cell (although often this current is set to zero) and the resulting intracellular potential is measured. This mode allows neurons to fire action potentials naturally, with magnitudes between 50 and 100 mV. This mode also allows measurement of single millivolt-scale subthreshold activity.

The circuit components of a current-clamp amplifier are *1*) a voltage buffer or amplifier with low input-referred voltage noise that can drive an ADC and *2*) a programmable current source. Most traditional patch-clamp amplifiers use a unity-gain buffer for monitoring intracellular voltages. A noise floor <25 μV rms over a bandwidth of 10 kHz is desired for high signal quality.

We designed a DC-coupled current-clamp voltage amplifier using low-noise amplifier circuitry based on principles developed by Harrison and Charles (2003). A gain of 4 was incorporated to boost the signal before it is digitized by the ADC. We also designed transistor-based programmable current sources to inject positive or negative currents over a wide range from 5 pA to 128 nA.

In vitro whole cell patch clamping in HEK293FT cells. We performed whole cell patch-clamp recordings from HEK293FT cells (Invitrogen) using the PatchChip. The HEK293FT cells were maintained between 10 and 70% confluence in DMEM cell culture medium (Cellgro) and supplemented with 10% fetal bovine serum (Invitrogen), 1% penicillin/streptomycin (Cellgro), and 1% sodium pyruvate (BioWhittaker). One to 2 days before recording, cells were plated at 5–20% confluence on glass coverslips coated with Matrigel (BD Biosciences). For the recordings, the cells were kept in extracellular solution (Tyrode's solution) consisting of (mM) 125 NaCl, 2 KCl, 3 $CaCl_2$, 1 $MgCl_2$, 10 HEPES, and 30 glucose. The pH of Tyrode's solution was adjusted to 7.3 using NaOH, and the osmolarity was 305 mosM. Patch pipettes with resistances of 4–6 MΩ were pulled from borosilicate glass capillaries (Warner Instruments) using a P97 pipette puller (Sutter Instrument, Novato, CA). The pipettes were filled with intracellular solution consisting of (in mM) 135 potassium gluconate (with more added empirically at the end, to bring osmolarity up to $\sim$290 mosM), 0.1 $CaCl_2$, 0.6 $MgCl_2$, 1 EGTA, 10 HEPES, 4 MgATP, 0.4 Na_2GTP, and 8 NaCl (pH adjusted to 7.2 by addition of KOH) as described previously (Klapoetke et al. 2014).

In vitro whole cell patch clamping in cultured neurons. All animal procedures were approved by the Committee on Animal Care at the Massachusetts Institute of Technology. Primary hippocampal neuronal cultures were prepared from embryonic *day 18* mouse embryos as previously described (Chen and Bear 2007). Hippocampi were dissected in ice-cold dissociation medium and digested in 0.01% papain for 1 h at 37°C. Neurons were triturated with a siliconized Pasteur pipette and then plated onto 12-mm glass coverslips coated with poly-lysine. Culture media consisted of Neurobasal A, 2% B27 supplement, 100 U/ml penicillin, 100 μg/ml streptomycin, and 0.5 mM L-glutamine. In a subset of experiments, a sodium channel blocker (1 μM TTX) was added to inhibit action potential generation. Cultures were maintained at 37°C in a humidified incubator gassed with 95% air and 5% CO_2. The pipette internal solution for current-clamp recordings contained 20 mM KCl, 100 mM Na-gluconate, 10 mM HEPES, 4 mM MgATP, 0.3 mM Na_2GTP, 7 mM phosphocreatine-Tris, and 0.2% biocytin with pH adjusted to 7.2 and osmolarity adjusted to 300 mosM; the internal solution for voltage-clamp contained 103 mM Cs-gluconate, 5 mM tetraethylammonium-Cl, 2.8 mM NaCl, 20 mM HEPES, 0.3 mM Na_2GTP, 4 mM MgATP, 10 mM Na_2-phosphocreatine, 0.2 mM EGTA, 0.2% biocytin, and 5 mM QX-314-Cl with pH adjusted to 7.2 and osmolarity adjusted to 300 mosM with sucrose or ddH_2O.

In vivo whole cell patch clamping. All animal procedures were approved by the Institutional Animal Care and Use Committee at the Georgia Institute of Technology. Methodology to perform automated whole cell patch-clamp electrophysiology has been previously described (Kodandaramaiah et al. 2012). Briefly, an adult male C57/BL6 mouse, 8 wk old, was anesthetized using a cocktail of ketamine and xylazine initially at 100 and 10 mg/kg, respectively, and redosed at 30- to 45-min intervals with 10–15% of the initial ketamine dose as needed if the animal was responsive to toe pinch. The subject was affixed in a stereotaxic apparatus (Kopf) and a head plate implant attached, followed by opening of a craniotomy 1 mm wide above the barrel cortex (centered 0.83 mm posterior and 3.0 mm lateral to bregma) using previously described protocols (Kodandaramaiah et al. 2012; Margrie et al. 2002). Once opened, the craniotomy was superfused with sterile saline throughout the experiment to keep the tissue moist. The anesthetized animal was then head-fixed using a custom three-dimensionally printed holder. Pipette solution was the same as in the in vitro preparation. Pipette capacitance was compensated in voltage clamp. No bridge balance compensation was performed.

RESULTS

Benchtop testing. We designed and fabricated the PatchChip in a commercially available 0.35-μm silicon CMOS process. We used an "analog-friendly" process that allowed for the fabrication of high-quality capacitors and resistors in addition to standard transistors that are used to build analog and digital circuits. The 0.35-μm feature size was smaller than the 0.5-μm feature size used by previously published patch-clamp micro-

circuits (Goldstein et al. 2011; Laiwalla et al. 2006; Sigworth 1995; Weerakoon et al. 2010) and offered higher performance due to smaller transistor gate lengths and lower threshold voltages.

Each microfabricated PatchChip (Fig. 3*A*) is 4.7 × 3.0 mm in size and contains more than 20,000 transistors, resistors, and capacitors. The chips were packaged in standard plastic leaded chip carrier (PLCC) packages to facilitate standard solder assembly onto circuit boards.

A custom-printed circuit board (PCB) was designed to connect the PatchChip to supporting circuits including voltage regulators and a 16-bit ADC. The PCB was placed inside a grounded aluminum case to provide Faraday shielding from interference and other sources of noise. A 7/16-20 threaded connector or a coaxial connector (pictured in Fig. 3*B*) was attached to the case to interface with commonly used pipette holders. This complete assembly acted as a head stage where the patch pipettes were mounted. Two connectors on the right side of the case provided connection points for interface cables that delivered power and digital signals to and from the PCB. These cables connected to a small USB interface board that allowed the PatchChip to be controlled and monitored by a host computer over a standard USB cable. Digital commands configured the patch-clamp electronics and selected amplifier modes and voltage/current-clamp values.

We also developed custom GUI software that allowed users to easily control the PatchChip. All software was written in C++ using the open-source Qt libraries (Qt Project Hosting, Oslo, Norway) to allow for cross-platform compilation under Windows, Mac, or Linux operating systems.

The interface software allows users to control and monitor voltage-clamp and current-clamp experiments. For example, users can apply voltage steps and measure the resulting time-varying currents (in voltage-clamp mode) or apply current steps and record the intracellular voltage (in current-clamp mode). Measured current or voltage waveforms can be saved to disk, and software was developed to load these data files into MATLAB (The MathWorks, Natick, MA). Multiple copies of the circuit board were built and used at various laboratories in different experimental settings, and the software was run on various computers. Both the hardware and software performed robustly in all settings.

The PatchChip is able to resolve voltages down to 8.2 μV and currents as small as 1.1 pA (Table 1). This is an improvement over the previously published chip (Goldstein et al. 2011; Weerakoon et al. 2010) and compares favorably with commercial patch-clamp amplifiers already on the market. For example, the commonly used Axopatch 200B patch-clamp amplifier from Molecular Devices (Sunnyvale, CA) has a current noise floor of 0.65 pA rms in high-gain

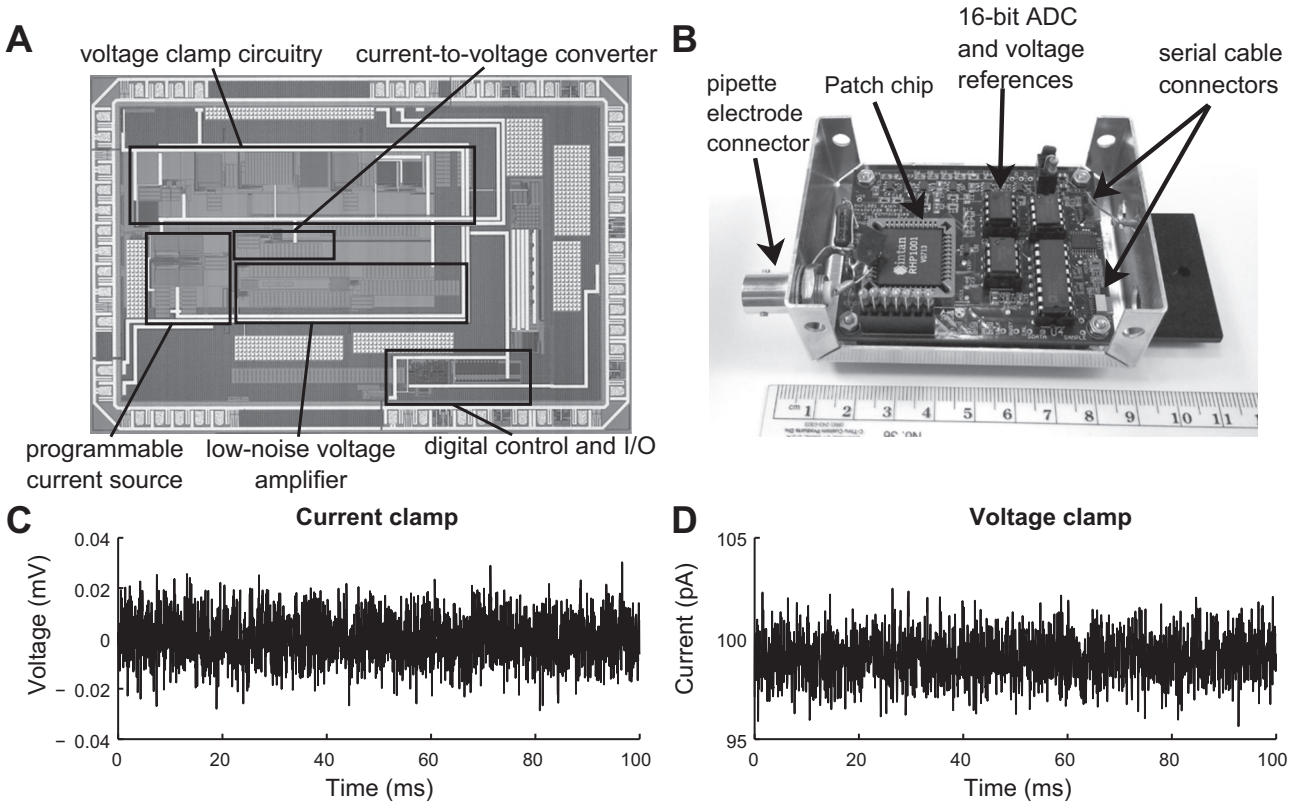

Fig. 3. PatchChip design and benchtop characteristics. *A*: microphotograph of the PatchChip. Each silicon chip measures 4.7 × 3.0 mm and contains more than 20,000 transistors, resistors, and capacitors. *B*: circuit board containing the PatchChip [in black plastic leaded chip carrier (PLCC) package labeled "Intan"] and supporting components. The aluminum enclosure (measuring 8.5 × 5.7 × 2.9 cm) shields the sensitive electronics from interference. This circuit board contains the functionality of the head stage as well as the rack-mounted amplifier and analog-to-digital converter (ADC) in traditional patch-clamp amplifier systems. All current and voltage measurements are digitized on this circuit board and passed to a USB interface board over digital serial cables. *C*: measured voltage noise floor of PatchChip in current-clamp (injected $I = 0$) mode. Noise over the 10-kHz bandwidth was 8.2 μV root mean square (rms). *D*: measured current noise floor of PatchChip in voltage-clamp mode measuring 100 pA in current. Noise over the 5-kHz bandwidth was 1.1 pA rms.

Table 1. *Electrical characteristics of existing patch-clamp amplifiers*

Parameter	Axopatch 200B or Axoclamp 900A (Molecular Devices)	Weerakoon et al. 2010 and Goldstein et al. 2011	PatchChip
Noise floor for current measurements (voltage clamp)	0.65 pA rms over 5 kHz (high gain) 1.65 pA rms over 5 kHz (low gain)	8 pA rms over 10 kHz	1.1 pA rms over 5 kHz
Noise floor for voltage measurements (current clamp)	23 μV rms over 10 kHz	150 μV rms over 5 kHz	8.2 μV rms over 10 kHz
Series resistance compensation	0–100 MΩ	0–80 MΩ	0–32 MΩ
Capacitance compensation	0–10 pF	0–10 pF	0–10 pF

mode or 1.65 pA rms in low-gain mode when the bandwidth is set to 5 kHz. This is comparable to our noise floor of 1.1 pA rms across 5 kHz as measured in voltage-clamp mode over 100 ms (Fig. 3*C*). The Axoclamp 900A microelectrode amplifier, also from Molecular Devices, has a voltage noise floor of 23 μV rms across a 10-kHz bandwidth in current-clamp mode. Our noise floor is nearly three times lower, at 8.2 μV rms across 10 kHz as measured in current-clamp mode over 100 ms (Fig. 3*D*).

To assess the effectiveness of the temperature calibration, we connected PatchChip to a 1.0-GΩ resistor and clamped the voltage across the resistor to 100 mV, producing a 100-pA set current. The output of the voltage-clamp current measurement circuitry was recorded along with the on-chip temperature sensor reading while the chip underwent a change in temperature from 3.5 to 24.5°C. When left uncorrected, the current measurements are strongly dependent on temperature (Fig. 4*A*); however, this relationship is accurately fit (Pearson's correlation coefficient, $r = 0.99$, $P < 0.01$) using a second-order polynomial. Use of this function to correct for temperature yields current measurements that are accurate to $\pm$3% across this 21°C temperature range; we expect this relationship to continue for higher temperatures, such as typical body temperatures, as well. Long-term drift and stability of the voltage-clamp circuit was measured across 2 h in a constant-temperature environment. The current measurements were found to stay within $\pm$3% of the true value over this period of time (Fig. 4*B*).

In vitro testing. The PatchChip head stage was mounted on a motorized manipulator (Sutter Instrument) and integrated with a standard inverted microscope for in vitro patch-clamping experiments (Fig. 5*A*). We first performed voltage-clamp and current-clamp experiments on cultured HEK293FT cells. The PatchChip was set to voltage-clamp mode, and the resistance of the pipette was monitored in real time by using the interface software to determine when the electrode tip had contacted a cell and a gigaseal (a tight electrical and mechanical seal with >1 GΩ of resistance to the extracellular fluid) had formed. After a gigaseal was obtained, either a short suction pulse or a high-amplitude voltage pulse (1 V, 1.0 ms) from the PatchChip was used to break the cell membrane at the electrode contact point to attain a whole cell configuration. Representative currents measured from a voltage-clamped HEK293FT cell are comparable to those measured using standard commercially available patch-clamp amplifiers (Fig. 5*B*).

In a similar fashion, we performed whole cell patch-clamp measurements on cultured neurons (Fig. 5*C*). Representative traces of membrane potential voltages from a whole cell patch-clamped neuron (access resistance, $R_a = 22$ MΩ; membrane resistance, $R_m = 274$ MΩ; membrane time constant, $\tau = 12.8$ ms; membrane capacitance, $C_m = 46.7$ pF) were measured in current-clamp mode in response to injected currents ranging from -100 to $+150$ pA (Fig. 5*D*). Current injection above 75 pA resulted in the cells being depolarized above threshold, leading to action potential firing. In an extended current-clamp experiment, the spontaneous membrane potential changes were recorded while a constant current ($I = -30$ pA) was injected (Fig. 5*E*). The cell fired action potentials at a rate of roughly 10 Hz, a physiologically realistic firing rate. Figure 5*F* shows a representative current trace from the same neuron when it was voltage clamped near its resting potential of -70 mV. Miniature postsynaptic currents with average peak

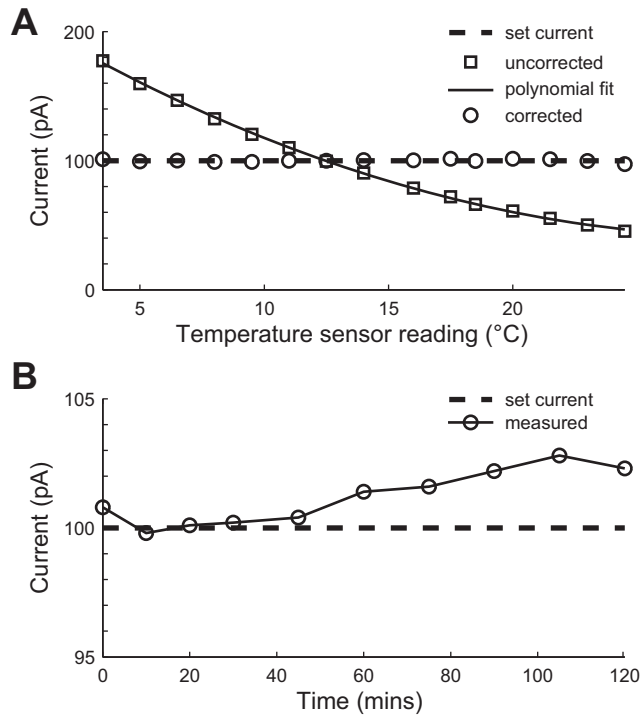

Fig. 4. Temperature-dependent and time-dependent voltage-clamp measurements. A 1-GΩ resistor was voltage clamped at 100 mV, producing a set current of 100 pA (dashed line). *A*: correction of temperature-dependent voltage-clamp measurements. The uncorrected current measurements (squares) vary predictably with temperature. A second-order polynomial (solid line) is used to correct the measurements based on the reading from the on-chip temperature sensor. The corrected measurements (circles) lie within $\pm$3% of the true current over a temperature change of 21°C. *B*: time drift of voltage-clamp measurements. Over a period of 120 min, the measured current deviated by less than $\pm$3% (circles) from the set current (dashed line).

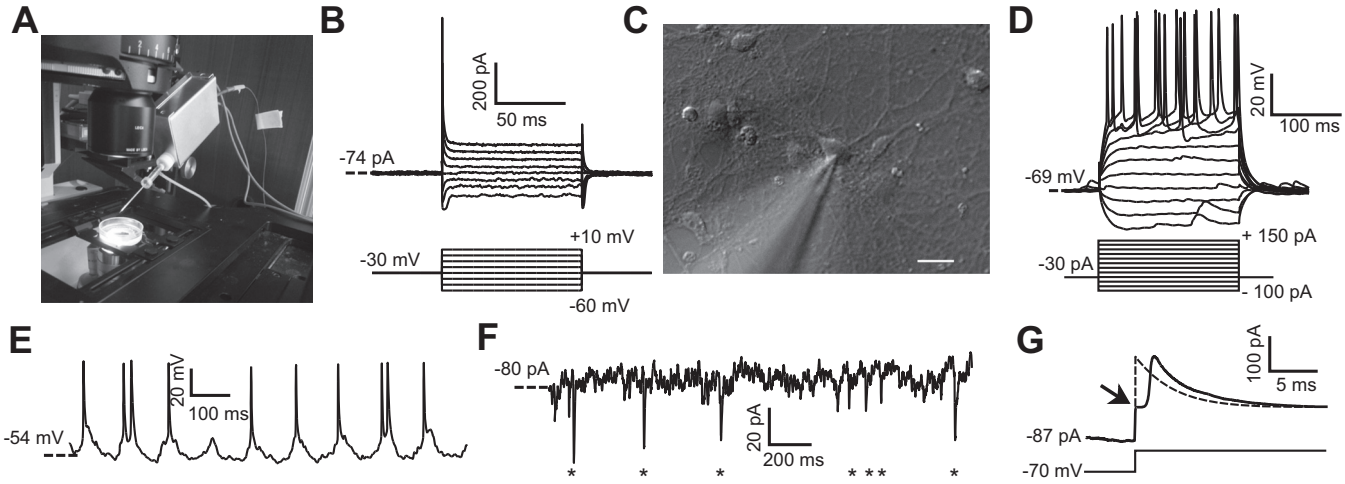

Fig. 5. In vitro PatchChip performance. *A*: PatchChip (inside aluminum box with blue interface cables) with glass pipette electrode connected. The blue cables convey power and digital data between the PatchChip circuitry and a host computer. The dish contains cultured HEK293FT cells. The PatchChip module is attached to a 3-axis micropositioner that allows the electrode tip to precisely contact a cell. *B*: HEK293FT voltage-clamp experiments using the PatchChip. Ionic currents were recorded in whole cell mode (*top*) in response to different command voltages (*bottom*). Current levels and time constants are consistent with typical HEK293FT cell characteristics. *C*: microscope view showing the tip of the glass pipette contacting a cultured neuron. The pipette was connected to the PatchChip, and voltage- and current-clamp experiments were performed on the cell. Scale bar, 10 μm. *D*: current-clamp experiment using the PatchChip. Action potentials were evoked when the injected current exceeded 75 pA. *E*: in vitro current-clamp recordings from cultured neurons using the PatchChip. A clamping current of -30 pA was injected into the cell. Spontaneous action potentials firing at a physiological rate are visible in the measured voltage waveform. *F*: voltage-clamp experiment using the PatchChip. The cell was held near its resting potential of -70 mV. Miniature postsynaptic currents in the picoamp range from spontaneous activity are visible (asterisks). *G*: crossover distortion in the voltage-clamp circuit when measured current switched direction. Passive membrane characteristics of a neuron were measured by using sodium channel blockers and stepping the control voltage from -70 to -40 mV. Arrow indicates a "kink" artifact lasting $\sim$1.4 ms that occurred due to crossover distortion. The ideal passive response of a cell to this voltage step is a first-order exponential (dashed).

amplitude of 23 $\pm$ 11.8 pA (mean $\pm$ SE; $n = 7$) and mean decay time of 4.8 $\pm$ 1.8 ms ($n = 7$) are observed at time points indicated by the asterisks plotted along the time axis (Fig. 5*F*). These results demonstrate the ability of the PatchChip to perform millisecond time resolution measurements of subthreshold synaptic events, as well as suprathreshold spiking events from single neurons in vitro, and can thus be used for a wide range of electrophysiological characterizations of excitable cells.

A limitation in the current implementation of the PatchChip is the crossover distortion that occurs when the measured current changes direction during voltage clamp. When current changes direction, the output of the op amp (Fig. 2, *A* and *B*) cannot switch instantaneously between the two feedback diodes (M1 and M2 in Fig. 2*B*). This creates a "kink" in the current measurement (duration = 1.4 ms), causing the response to deviate from the expected first-order exponential (Fig. 5*G*).

In vivo testing. The PatchChip was integrated with the "autopatcher," a robotic system that automatically performs in vivo patch clamping as demonstrated previously using commercially available amplifiers (Kodandaramaiah et al. 2012). We modified our existing software to incorporate autopatcher modules that allowed automated control of motor movement and pipette pressure. The PatchChip served as a custom head stage on an existing autopatcher setup (Fig. 6*A*). In one trial, on the initiation of the autopatcher algorithm, a neuron was found at a depth of 452 μm in the brain. A multigigaohm seal was achieved in $\sim$90 s (Fig. 6*B*). A whole cell configuration was achieved by "zapping," using a 1-V, 50-μs pulse for break-in. We performed both voltage-clamp and current-clamp measurements on the neuron (R_a = 72 MΩ, R_m = 120 MΩ, τ = 27.4 ms, C_m = 228 pF; Fig. 6*B*, *inset*, and *C*), observing action potentials when currents of 200 pA or more were injected into the cell.

DISCUSSION

We have designed and fabricated the PatchChip for patch-clamp electrophysiology using standard silicon fabrication processes and have tested it in HEK293FT cells, cultured neurons, and an in vivo mouse preparation. In these settings, the PatchChip performed whole cell patch-clamp measurements in both current- and voltage-clamp modes, which enabled detection of millisecond-timescale subthreshold events and suprathreshold action potential firing events from single neurons. These results demonstrate the versatility of the PatchChip in a variety of experimental settings.

The performance of the chip presented in this article is currently limited by crossover distortion and low series resistance compensation capability. The crossover distortion creates an artifact in the recording that alters current measurements that are near zero. Improvements to the bandwidth and slew rate of the op amp should reduce this effect. The PatchChip is also limited by its range of series resistance compensation, which goes up to 32 MΩ, although this also can be extended in future revisions. This is primarily a limitation for in vivo whole cell recordings in aged animals, where series resistance can reach over 100 MΩ (Margrie et al. 2002), and, to a lesser extent, for dendritic recordings (Stuart et al. 1993). On the other hand, when whole cell somatic recordings are performed in neuronal cultures (Hamill et al. 1981) and brain slices (Stuart et al. 1993), access resistance is typically $<$30 MΩ,

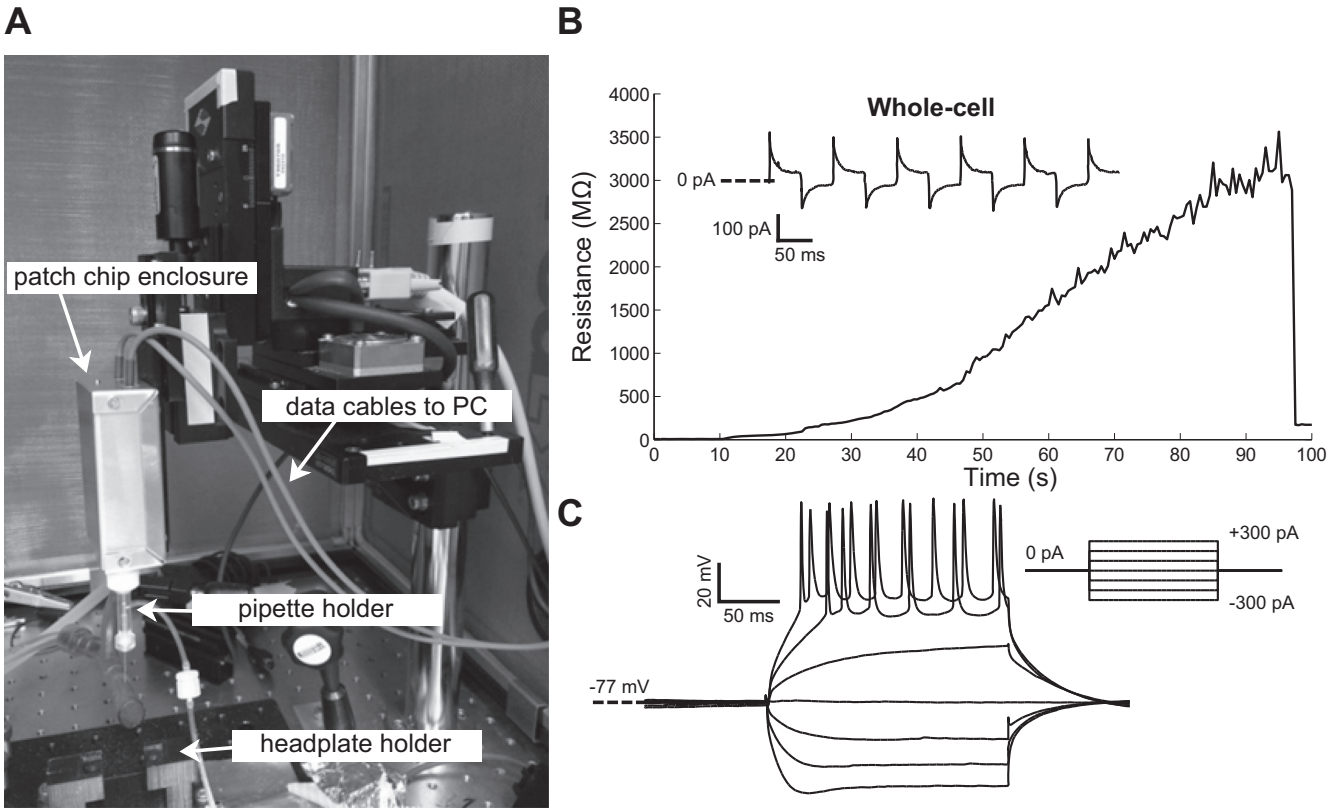

Fig. 6. In vivo PatchChip performance. *A*: the PatchChip (inside aluminum box with blue power/data cables) connected to the "autopatcher," an automated in vivo patch-clamping robot. *B*: pipette electrode resistance measured by the PatchChip during a 100-s in vivo autopatcher experiment in which a seal of >3 GΩ was achieved using an automated robotic system incorporating the PatchChip. Successful membrane break-in to achieve whole cell configurations occurred at $t = 97$ s. Current traces recorded in voltage clamp in response to +5-mV, 10-Hz square-wave pulses (holding potential −72 mV) show resistive-capacitive transients typical of a whole cell patch-clamped cell (*inset*). *C*: in vivo neuron current-clamp measurements taken with the PatchChip and autopatcher system from the neuron shown in *B*. Action potentials were visible when the injected current exceeded 100 pA.

which is within the range of series resistance compensation of the PatchChip.

The realization of an on-chip patch amplifier using standard silicon fabrication processes will dramatically drive down the cost and physical scale of patch-clamp instrumentation. Combining the PatchChip with recent advances in automation of the patch-clamp technique will greatly expand the market for patch-clamp instrumentation in both academia and industry. In particular, applications where a large number of simultaneous intracellular recordings are required continue to multiply as researchers aim to record intracellular signals from more and more neurons (Perin and Markram 2013). The availability of affordable, automated, multichannel patch-clamp instrumentation represents an innovative technology that has the potential to energize an already productive research area in neuroscience and medicine (Kodandaramaiah et al. 2013). Automated patch clamping has even recently been used in conjunction with optogenetic neural control, potentially enabling new ways of synapse-level circuit analysis (Chuong et al. 2014).

The PatchChip presented in this article will be refined and optimized, and multiple patch-clamp amplifiers will be fabricated on a single chip to serve emerging instrumentation requirements of highly scalable multichannel patch-clamp recording. In addition to scalability, this integrated electronic amplifier represents an enabling technology for benchtop commoditized patch-clamping systems.

GRANTS

R. R. Harrison acknowledges funding by National Institutes of Health (NIH) Grant 1R43NS083108-01. A. A. Chubykin, M. F. Bear, and E. S. Boyden acknowledge funding by The Simons Center for the Social Brain. E. S. Boyden acknowledges funding by NIH Grants 1R01EY023173, 1R01NS075421, and 1R01MH103910-01, the New York Stem Cell Foundation-Robertson Award, National Science Foundation (NSF) Award CBET 1053233, and the Institute of Engineering and Technology Harvey Prize. I. Kolb and C. R. Forest acknowledge the NIH Computational Neuroscience Training Grant DA032466-02. C. R. Forest acknowledges the NIH BRAIN Initiative Grant 1U01MH106027-01, the NIH Single Cell Grant 1R01EY023173, NSF Grants EHR 0965945 and CISE 1110947, Georgia Tech Translational Research Institute for Biomedical Engineering & Science (TRIBES) Seed Grant Awards Program, Georgia Tech Fund for Innovation in Research and Education (GT-FIRE), Wallace H. Coulter Translational/Clinical Research Grant Program, and support from Georgia Tech through the Institute for Bioengineering and Biosciences Junior Faculty Award, Technology Fee Fund, Invention Studio, and the George W. Woodruff School of Mechanical Engineering.

DISCLOSURES

R. R. Harrison is a co-founder of Intan Technologies and maintains equity in this company.

AUTHOR CONTRIBUTIONS

R.R.H. conception and design of research; R.R.H. and I.K. prepared figures; R.R.H. drafted manuscript; R.R.H., I.K., S.B.K., A.A.C., E.S.B., and C.F. edited and revised manuscript; R.R.H., I.K., S.B.K., A.A.C., A.Y., M.F.B., E.S.B., and C.F. approved final version of manuscript; I.K., S.B.K., A.A.C.,

and A.Y. performed experiments; I.K., S.B.K., and A.A.C. analyzed data; I.K., S.B.K., and A.A.C. interpreted results of experiments.

REFERENCES

Chen WS, Bear MF. Activity-dependent regulation of NR2B translation contributes to metaplasticity in mouse visual cortex. *Neuropharmacology* 52: 200–214, 2007.

Chuong AS, Miri ML, Busskamp V, Matthews GA, Acker LC, Sørensen AT, Young A, Klapoetke NC, Henninger MA, Kodandaramaiah SB, Ogawa M, Ramanlal SB, Bandler RC, Allen BD, Forest CR, Chow BY, Han X, Lin Y, Tye KM, Roska B, Cardin JA, Boyden ES. Noninvasive optical inhibition with a red-shifted microbial rhodopsin. *Nat Neurosci* 17: 1123–1129, 2014.

Goldstein B, Choe K, Sigworth FJ, Culurciello E. A four-channel integrated patch-clamp amplifier with current-clamp capability. *IEEE 54th International Midwest Symposium on Circuits and Systems (MWSCAS), Seoul, Korea, 2011*, p. 1–4.

Hamill OP, Marty A, Neher E, Sakmann B, Sigworth FJ. Improved patch-clamp techniques for high-resolution current recording from cells and cell-free membrane patches. *Pflügers Arch* 391: 85–100, 1981.

Harrison RR, Charles C. A low-power low-noise CMOS amplifier for neural recording applications. *IEEE J Solid-State Circuits* 38: 958–965, 2003.

Hodgkin AL, Huxley AF. A quantitative description of membrane current and its application to conduction and excitation in nerve. *J Physiol* 117: 500–544, 1952.

Klapoetke NC, Murata Y, Kim SS, Pulver SR, Birdsey-Benson A, Cho YK, Morimoto TK, Chuong AS, Carpenter EJ, Tian Z, Wang J, Xie Y, Yan Z, Zhang Y, Chow BY, Surek B, Melkonian M, Jayaraman V, Constantine-Paton M, Wong GK, Boyden ES. Independent optical excitation of distinct neural populations. *Nat Methods* 11: 338–346, 2014.

Kodandaramaiah SB, Boyden ES, Forest CR. In vivo robotics: the automation of neuroscience and other intact-system biological fields. *Ann NY Acad Sci* 1305: 63–71, 2013.

Kodandaramaiah SB, Franzesi GT, Chow BY, Boyden ES, Forest CR. Automated whole-cell patch-clamp electrophysiology of neurons in vivo. *Nat Methods* 9: 585–587, 2012.

Laiwalla F, Klemic KG, Sigworth FJ, Culurciello E. An integrated patch-clamp amplifier in silicon-on-sapphire CMOS. *IEEE Trans Circuits Syst I Regul Pap* 53: 2364–2370, 2006.

Margrie TW, Brecht M, Sakmann B. In vivo, low-resistance, whole-cell recordings from neurons in the anaesthetized and awake mammalian brain. *Pflügers Arch* 444: 491–498, 2002.

Mead C. *Analog VLSI and Neural Systems*. Boston, MA: Addison-Wesley Longman, 1989.

Molecular Devices. *Axon Axoclamp 900A Microelectrode Amplifier* (Online). http://www.moleculardevices.com/products/instruments/axon-patch-clamp/axon-axoclamp.html [23 Jun 2014a].

Molecular Devices. *Axon Axopatch 200B Capacitor Feedback Patch Clamp Amplifier* (Online). http://www.moleculardevices.com/products/instruments/axon-patch-clamp/axon-axopatch.html [23 Jun 2014b].

Molleman A. Whole-cell protocols and data analysis. In: *Patch Clamping: An Introductory Guide to Patch Clamp Electrophysiology*. Chichester, UK: John Wiley & Sons, 2002, p. 115–139.

Neher E, Sakmann B. Single-channel currents recorded from membrane of denervated frog muscle fibres. *Nature* 260: 799–802, 1976.

Perin R, Markram H. A Computer-assisted Multi-electrode Patch-clamp System. *J Vis Exp*, 2013.

Safronov BV, Vogel W. Electrical activity of individual neurons: patch-clamp techniques. In: *Modern Techniques in Neuroscience Research*, edited by Windhorst PD, Johansson PD. Berlin: Springer, 1999, p. 173–192.

Sakmann B, Neher E. *Single-Channel Recording* (2nd ed.). New York: Springer, 2009.

Sigworth FJ. Design of the EPC-9, a computer-controlled patch-clamp amplifier. 1. Hardware. *J Neurosci Methods* 56: 195–202, 1995.

Stuart GJ, Dodt HU, Sakmann B. Patch-clamp recordings from the soma and dendrites of neurons in brain slices using infrared video microscopy. *Pflügers Arch* 423: 511–518, 1993.

Tuthill M. A switched-current, switched-capacitor temperature sensor in 0.6-μm CMOS. *IEEE J Solid-State Circuits* 33: 1117–1122, 1998.

Vittoz E, Fellrath J. CMOS analog integrated circuits based on weak inversion operations. *IEEE J Solid-State Circuits* 12: 224–231, 1977.

Weerakoon P, Culurciello E, Yang Y, Santos-Sacchi J, Kindlmann PJ, Sigworth FJ. Patch-clamp amplifiers on a chip. *J Neurosci Methods* 192: 187–192, 2010.